

博士論文 (要約)

Analysis on the functions of ubiquitin-proteasome-pathway
factors in porcine oocyte maturation process

(ユビキチン/プロテアソーム経路関連因子のブタ卵成熟過程における機能の解析)

Fujioka Yoshie

藤岡良江

Laboratory of Applied Genetics

Department of Animal Resource Sciences

The University of Tokyo

Contents

General Introduction	1
Figure	5
Chapter 1: Function of EMI in porcine oocyte maturation	
Introduction	7
Materials and Methods	9
Results	13
(1) EMI overexpression by Flag- <i>EMI</i> mRNA injection and expression inhibition by <i>EMI</i> asRNA injection	
(2) Influences of RNA injection on porcine oocyte maturation	
(3) Effects of up- or downregulation of EMI on the GVBD of porcine oocyte maturation	
(4) Effects of up- or downregulation of EMI after GVBD and MII arrest of porcine oocytes	
Discussion	18
Figures	22

Chapter 2:

本章の内容は学術雑誌論文として出版する計画があるため、公表できない。5年以内に出版予定。

Chapter 3:

本章の内容は学術雑誌論文として出版する計画があるため、公表できない。5年以内に出版予定。

General Discussion

本章の内容は学術雑誌論文として出版する計画があるため、公表できない。5年以内に出版予定。

Appendix

本章の内容は学術雑誌論文として出版する計画があるため、公表できない。5年以内に出版予定。

References

General Introduction

In ovarian follicles, vertebrate oocytes are arrested at first meiotic prophase which contains large nucleus called germinal vesicle (GV). In order for oocytes to be ready for fertilization, oocytes must go through meiotic process until second meiotic metaphase (MII). This meiotic process called oocyte maturation is initiated by rise in maturation/M phase promoting factor (MPF) activity (Masui and Markert, 1971). MPF is the complex composed of catalytic subunit, cyclin dependent kinase 1 (CDK1), and regulatory subunit, cyclin B (CCNB) (Draetta et al., 1989). Not until these subunits combine to make a complex, CDK1 cannot be active as MPF. It is commonly known that the amount of CDK1 protein does not oscillate much, leaving the regulation of MPF activity to ways other than controlling of CDK1 protein accumulation. One way of regulating MPF activity is by controlling CCNB accumulation. The accumulation of CCNB orchestrates the progression of oocyte maturation (Fig. 0A). As noted above, vertebrate oocytes in ovarian follicles are arrested at the stage where they contain GV (GV stage) with low MPF activity. From this stage onward, CCNB starts to accumulate within oocytes by hormonal stimulation or isolation of follicles, coinciding with the rise of MPF activity (Hoffmann et al., 2006; Sagata, 1996). This accumulation of CCNB triggers GV to break its vesicular membrane (germinal vesicle breakdown; GVBD) and initiate oocyte maturation process. As CCNB continues to accumulate, oocyte reaches to prometaphase of first meiosis (PMI), and the accumulation reaches peak at first meiotic metaphase (MI). Then CCNB is rapidly degraded, making oocytes to progress through first meiotic anaphase-telophase (A-TI) (Chang et al., 2003). After the transient decline of CCNB accumulation, CCNB again starts to be accumulated and the accumulation reaches plateau when oocytes reach to MII. At this stage, oocytes become ready for fertilization and until being fertilized, oocytes remain at MII.

Like the oscillation of CCNB accumulation in oocyte maturation, the accumulation of various proteins is being controlled by protein degradation systems. One typical system of protein degradation is a ubiquitin-proteasome pathway (UPP). UPP is a protein-catabolism mechanism in which proteasome, a 26S protein-complex with 20S catalytic-core, degrades the ubiquitinated target substrate (Eytan et al., 1989). For certain protein to be degraded through UPP, target protein must be ubiquitinated. The ubiquitination of a target protein is mediated by ubiquitin-activating enzyme (E1), ubiquitin-conjugating enzyme (E2), and ubiquitin ligase (E3) (Fig. 0B). These three enzymes work in line to have protein ubiquitinated: first, free ubiquitin is bound to E1, second, ubiquitin is passed over to E2, and third, ubiquitin is transferred to E3. Then finally, E3 conjugates ubiquitin to target substrate (Hershko et al., 1983; Ciechanover et al., 1982; Kleiger and Mayor, 2014). Since ubiquitination must be highly specific to selectively ubiquitinate target substrate, many different E1, E2, and E3 enzymes exist (Deshaies and Joazeiro, 2009; Kleiger and Mayor, 2014). For example, among the various E2s and E3s, the degradation of CCNB is mediated by UBE2C and UBE2S as E2, and anaphase-promoting-complex/cyclosome (APC/C) as E3 (Fig. 0B) (Peters, et al., 2002). For APC/C, there exist a specific inhibitor, early mitotic inhibitor 1 and 2 (EMI1 and EMI2), which prevents APC/C from conjugating ubiquitin onto the target protein. EMI1 and EMI2 are known to function with CCNB accumulation and studies are conducted on *Xenopus* and mouse oocytes about their roles in oocyte maturation. Overexpression of EMI1 in mouse prophase oocytes leads to the stabilization of CCNB and triggers early GVBD while inhibition of EMI1 enhances CCNB destruction and delays GVBD (Marangos et al., 2006). Existence of EMI1 in *Xenopus* oocytes remains controversial with some report confirming the existence and others denying it (Ohe et al., 2007; Ohsumi et al., 2004; Schmidt et al., 2004; Tung et al., 2004; Zachariae, 2005). In both *Xenopus* and

mouse, EMI2 is known to be a cytostatic factor (CSF), which withholds oocytes in MII until fertilization and prevent the formation of pronucleus (PN) (Ohsumi et al., 2004; Tung et al., 2004). UBE2C and UBE2S are E2 enzymes which function in line with APC/C to ubiquitinate CCNB (Dimova et al., 2012; Kirkpatrick et al., 2006). Though both UBE2C and UBE2S are E2, their roles are not interchangeable: UBE2C is known to be involved in ubiquitin monomer formation by passing the first ubiquitin to be conjugated to target protein (mono-ubiquitination) and UBE2S is mainly involved in ubiquitin chain elongation (poly-ubiquitination) (Jin et al., 2008; Ye and Rape, 2011). Therefore, as in vitro study has revealed, UBE2S alone cannot initiate ubiquitin chain formation but only elongates the chain which is created by UBE2C (Garnett et al., 2009; Wu et al., 2010). These E2 and E3, together with E3 inhibitors, regulate CCNB degradation via UPP.

Although the knowledge about the contribution of EMI and UBE2 to the oocyte maturation had been unraveled in *Xenopus* and mouse, these examinations had been focusing on one aspect of oocyte maturation such as only GVBD, only the spindle formation in MI or only meiotic arrest in MII. Therefore, no single conclusive notion can be drawn for the function of EMI and UBE2 concerning oocyte maturation process. In addition, because mouse oocytes are somewhat unique in the sense that it does not require protein synthesis for GVBD and it requires much less time for the completion of maturation, the research result of mouse oocytes cannot be simply applied to mammals as a whole (Schultz and Wassarman, 1977; Hampl and Eppig, 1995). Despite these facts, mouse is currently the only mammalian species which these factors have been examined, and thus it still needs investigations to reveal the function of those factors in oocyte maturation of mammalian specie other than mouse.

Porcine oocytes are suitable candidate to do a research on oocyte maturation. In the case of porcine oocytes, like other mammals, porcine oocytes require protein

synthesis for triggering GVBD (Fulka et al., 1986). Furthermore, compared to other non-model-organism species, large amounts of uniform oocytes can be obtained from pigs of commercial slaughterhouse. In addition to this, factors and mechanisms surrounding porcine oocyte maturation is well delineated, making a comprehensive interpretation of the experiment results possible. Thus, in this study, I used porcine oocytes and investigated how EMI and UBE2 affect oocyte maturation to unravel the contribution of these factors to the mammalian oocyte maturation.

In the present study, I investigated the functions and roles of UPP factors, EMI1, EMI2, UBE2C, and UBE2S, on the progression of mammalian oocyte maturation by the reverse genetic methods, in which I overexpressed or downregulated these factors by injecting mRNA or antisense RNA (asRNA), respectively. I focused on EMI functions in chapter 1, and UBE2 functions in chapter 2. In chapter 3, I focused on and further investigated the result obtained in chapter 2; the precocious GVBD triggered by UBE2S overexpression.

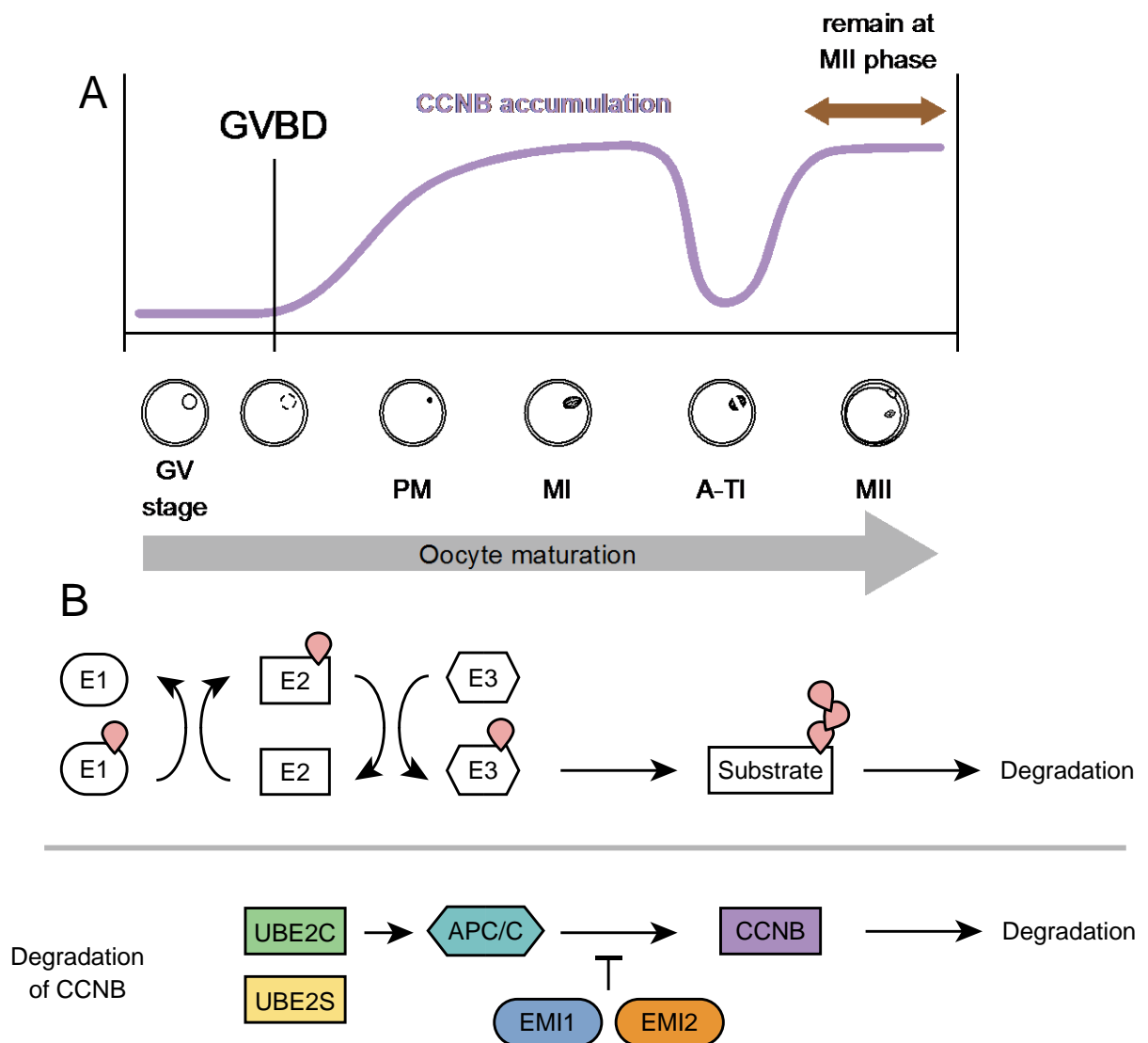


Fig.0 Oocyte maturation process and ubiquitin-proteasome pathway (UPP)

(A) The schematic drawing of CCNB accumulation during oocyte maturation. GV: germinal vesicle; GVBD, germinal vesicle breakdown; PM, first meiotic prometaphase; MI, first meiotic metaphase; A-TI, first meiotic anaphase-telophase; MII, second meiotic metaphase. (B) Protein degradation through UPP. E1: ubiquitin-activating enzyme, E2: ubiquitin-conjugating enzyme, E3: ubiquitin ligase.

Chapter 1

Functions of EMI in porcine oocyte maturation

Introduction

As noted in the general introduction, EMI is the inhibitor of APC/C and several studies have shown their involvement in M phase progression including oocyte maturation (Hsu et al., 2002; Margottin-Goguet et al., 2003; Ohsumi et al., 2004). Although EMI1 and EMI2 have similar structural characteristics with domain conformation and a region involved in APC/C inhibition (Yamano, 2013), several studies have reported differences in their expression patterns and physiological roles.

EMI1 was originally identified in *Xenopus* oocytes as cytostatic factor (CSF) which prevented CCNB degradation in mature oocytes and induced MII arrest until fertilization (Reimann et al., 2001; Reimann et al., 2002). However, later studies revealed the cross-reactivity of the EMI1 antibodies, and at present, cross-reacted EMI2 is recognized as the genuine CSF (Ohsumi et al., 2004; Tung et al., 2005). It has been reported in *Xenopus* and mouse that only EMI2 inhibition resulted in a decrease of CCNB level in the MII oocytes and the escape of oocytes from MII arrest (Shoji et al., 2006). Conversely, the overexpression of EMI2 prevented the oocyte activation (Schmidt et al., 2005). Although EMI1 inhibition has been suggested to have no effects on MII arrest, the possible functions of EMI1 in MII arrest have never been evaluated in other than *Xenopus* and mouse oocytes.

As for the EMI1, when EMI1 is inhibited in mouse oocytes, CCNB accumulation is reduced in GV oocytes, resulting in the delay in GVBD, whereas EMI1 overexpression initiates GVBD (Shoji et al., 2006; Marangos et al., 2007). In contrast to EMI1 expression in mouse, existence of EMI1 in *Xenopus* oocytes remains controversial with some report confirming the existence and others denying it (Ohsumi et al., 2004; Tung et al., 2004). In addition to this, there are no reports investigating the functions of EMI1 and EMI2 in species other than *Xenopus* and mouse.

Based on the background noted above, I focused on the EMI functions in porcine oocyte maturation and the effects especially on the GVBD and MII arrest in porcine oocytes by overexpressing and downregulating EMI expression in porcine oocytes using RNA injection method. RNA injection method requires the template porcine EMI1 and EMI2 sequence, and for this purpose, I first cloned porcine EMI1 and EMI2 cDNA from porcine immature oocytes total RNA. Since no effective antibody was available to detect EMI1 or EMI2, mRNA was designed to contain Flag-tag and the detection was done by an anti-Flag antibody. Before assessing the effect of EMI regulation, the influence of RNA injection on oocyte maturation was evaluated using the oocytes injected with enhanced green fluorescent protein (EGFP) mRNA, which was co-injected with mRNA or asRNA for every injection performed. EGFP mRNA was co-injected as an indication of injection and of alive oocytes when oocytes were selected according to EGFP fluorescence after culture. The effects of EMI were assessed by nuclear states including pronuclear (PN) formation after parthenogenetic activation of oocytes using electronic stimulation and the protein detection, such as CCNB accumulation and phosphorylation of ribosomal S6 kinase (RSK), which phosphorylation state is the indication of mitogen-activated protein (MAP) kinase signaling pathway (Erikson and Maller, 1985; Sugiura et al., 2002). In addition to this, the effect of expression regulation on oocytes cultured in high cAMP environment was also assessed. Within the ovarian follicles, the cAMP concentration is maintained high, and thus, the oocytes cultured in high cAMP environment can be considered as the model of those in follicular environment. The effect of EMI on GV arrest oocytes in follicles was assessed with the RNA injection method.

Materials and Methods

Porcine oocyte culture

Prepubertal gilt ovaries were collected from commercial slaughterhouse and cumulus-oocyte complexes (COCs) were aspirated from the follicles of 2-5 mm in diameter. Collected COCs were washed in a culture medium, consisting of a modified Krebs-Ringer bicarbonate solution (TYH; Toyoda et al., 1971) containing 1.0 IU/mL eCG (Serotoropin; ASKA Pharmaceutical, Japan), and 20% porcine follicular fluid. The porcine follicular fluid was prepared as previously described (Naito et al., 1988); the aspirated fluid was centrifuged for 25 minutes at 1,300 g and the supernatant was collected as porcine follicular fluid, stored at -80 °C until use. About 25 COCs with intact cumulus cells were cultured in the above culture medium (100 µL) at 37 °C, saturated humidity, and 5% CO₂ in air. For cAMP supplied culture, 5 mM of 8-Br cAMP (Sigma-Aldrich, MO, USA) was added to the culture medium and oocytes were cultured for 48 h. After culture, cumulus cells were removed from oocytes by gentle pipetting in saline supplemented with 0.1% polyvinylpyrrolidone (PVP) and 0.1% hyaluronidase. Denuded oocytes were subjected to nucleus observation and Western blotting analysis. Nucleus states were observed with mounting denuded oocytes on a glass slid, fixed with acetic acid-ethanol (1:3), stained with 0.75% acetoorcein solution, washed with acetic acid : glycerin : distilled water (1:2:4), and then sealed with EUKITT (Mounting reagent; O. Kindler, Germany).

Cloning of EMI1 and EMI2 cDNAs and vector construction

Total RNA was extracted from non-cultured porcine oocytes using Trizol reagent (Invitrogen, CA, USA), and first-strand cDNA was synthesized with SuperScript III (Invitrogen) according to the manufacturer's instruction. Porcine EMI1 and EMI2 cDNAs

were amplified by PCR with a thermal cycler (GeneAtlas; ASTEC, Japan) using the primer sets designed from NCBI porcine EST database and Ensembl predicted gene sequence (appendix: Table 1). For mRNA preparation, each forward primer was designed to omit a start codon and added a BglII site before EMI1 or EMI2 sequence, and each reverse primer was designed at a downstream of stop codon with BglII site, in order to add a Flag-tag at the N-terminal. PCR fragments were cloned once into pGEM-T Easy vector (A1360; Promega, WI, USA) and then digested with BglII, then inserted into the BamHI-digested pCMV-Tag1 vector (Agilent Technologies, CA, USA). These vectors were referred to as *Flag-EMI1-vector* and *Flag-EMI2-vector*. For antisense RNA (asRNA) preparation, full-length EMI1 ORF and partial fragment of EMI2 ORF were also cloned using another primer sets (appendix: Table 1). The PCR products were cloned into a pGEM-T Easy vector and referred to as *EMI1-asRNA-vector*, and *EMI2-asRNA-vector*, respectively. Cloned products were sequenced with a commercial sequencing kit (Applied Biosystems, CA, USA) using a DNA sequencer (Applied Biosystems) following the manufacturer's instruction.

In vitro RNA synthesis

RNA was synthesized in vitro from the above vectors linearized by restriction enzymes, using either T3-, T7-, or Sp6- RNA polymerase (Promega) in the presence of m7G(5')ppp(5')G to synthesize capped RNA transcripts as described previously (Ohashi et al., 2001). The restriction enzymes and RNA polymerases used for each RNA synthesis are listed in the Table 2 (appendix: Table 2). Synthesized RNA was precipitated with ethanol, washed, dried, and then resuspended in RNase-free water (Gibco, NY, USA). Resuspended RNA solution was stored in -80 °C until use. Enhanced green fluorescent protein (EGFP) mRNA was synthesized in the same manner from EGFP vector (Ohashi et

al., 2001).

Microinjection

The concentration of RNA solution was adjusted to 250 ng/ μ L and was co-injected with 250 ng/ μ L of EGFP mRNA as an indicator of microinjection and oocyte viability. RNA was microinjected to the COCs placed in 35 μ L of the culture medium using microinjectors (MO-202U; Narishige, Japan) equipped with manipulators (GJ-8; Narishige) mounted on inverted microscope (Diaphot 200; Nikon, Japan). Approximately 50 pL of RNA solution was injected to the cytoplasm of non-cultured (GV) or 42 h cultured (MII) oocytes by continuous pneumatic pressure. For MII oocyte injection, cultured COCs were denuded in the culture medium supplied with 0.1% hyaluronidase prior to the injection. The injected oocytes were cultured as described above up to 48 h. Cultured oocytes were selected by EGFP fluorescence observed under fluorescent microscope and selected oocytes were subjected to further analysis.

Parthenogenetic activation

After 48 h maturation culture, COCs were denuded and put in a mannitol solution (0.3 M mannitol, 0.1 mM MgSO₄, 0.05 mM CaCl₂, 0.01% PVA). Activation was performed with single DC pulse (150 V/mm for 0.99 μ sec) and oocytes were cultured for 24 h in the culture medium.

Western blotting analysis

The micro-Western blot was performed as described in previous report (Naito et al., 1999). Oocyte number used for each experiment is indicated in figure legends. Antibodies used were: anti-RSK (sc-231-G, goat IgG polyclonal antibody; Santa Cruz, TX,

USA), anti-CCNB1 (ADI-KAM-CC195-E, mouse IgG monoclonal antibody; Enzo Life Sciences, Germany), anti-Cdc2 (sc-54, mouse IgG monoclonal antibody; Santa Cruz), and anti-Flag (F1804, mouse IgG monoclonal antibody; Sigma-Aldrich). Each antibody was reacted with either horseradish peroxidase (HRP)-conjugated anti-mouse IgG (Jackson ImmunoResearch Laboratories, PA, USA) or HRP-conjugated anti-goat IgG (Jackson ImmunoResearch Laboratories). Signals were detected using ImmunoStar LD (Wako, Japan) and C-Digit (Li-Cor; Lincoln, NE, USA) as instructed by manufacturer. Relative intensity of detected signals was quantified using Image-J software if necessary.

Statistical analysis

Data were analyzed with Chi-square test and probability of $p < 0.05$ was considered as statistically significant.

Results

(1) EMI overexpression by Flag-EMI mRNA injection and expression inhibition by EMI asRNA injection

Overexpression of EMI was confirmed with Flag-EMI mRNA injected oocytes by Western blotting using an anti-Flag antibody. Specific Flag-EMI1 and Flag-EMI2 bands were detected (Fig.1.1). The inhibitory effect of each asRNA and its specificity on protein synthesis was evaluated by co-injecting *EMI1* and *EMI2* asRNA with one of the Flag-EMI mRNAs and examining the change in Flag signals. The Flag signal intensity of only the target EMI was decreased by each asRNA co-injection (Fig. 1.1), showing the effectiveness of *EMI* asRNA injection and its specificity on the downregulation of EMI expression.

(2) Influences of RNA injection on porcine oocyte maturation

The GVBD and MII rates of no-injection and EGFP mRNA injected oocytes were examined for the indicated periods (Fig.1.2). The observation revealed that GVBD started at 18 h of culture then reached maximum level at 24 h and did not increase until 48 h in both groups (Fig. 1.2A). Most of oocytes reached MII within 48 h and arrested until 72h (Fig.1.2B), confirming the result of the previous studies (Nishimura et al., 2010; Ohashi et al., 2003; Yamamuro et al., 2008). There was no difference between no-injection and EGFP mRNA injected oocytes in either GVBD or MII rate except for the GVBD rate at 18 h of culture where the rate of EGFP mRNA injected oocytes were significantly higher than that of no-injection oocytes. Considering these result, I used not only EGFP mRNA injected oocytes but also no-injection oocytes as a control except for the oocytes cultured for 18 h.

(3) Effects of up- or downregulation of EMI on the GVBD of porcine oocyte maturation

To investigate the functions of porcine EMI in GVBD, EMI was first overexpressed by injecting Flag-*EMI* mRNA to GV stage oocytes and the meiotic progression of the oocytes were observed. Most of the EGFP mRNA-injected oocytes were at the GV stage until 12 h and GVBD occurred at 24 h of culture, whereas Flag-*EMI1* and -*EMI2* mRNA-injected oocytes underwent GVBD at 9 h and 12 h, respectively (Fig.1.3A). Next, the effect of EMI downregulation on GVBD was assessed by injecting asRNA and the GVBD rate of oocytes were observed after 18 h of culture (Fig. 1.3B). *EMI1* downregulated oocytes displayed lower GVBD rate compared to EGFP mRNA-injected oocytes whereas *EMI2* downregulation had no effect. This result indicated that only *EMI1* plays positive roles in the GVBD of porcine oocytes.

Western blotting was performed next to confirm the observed GVBD rates of Flag-*EMI* mRNA-injected oocytes. It was confirmed by detecting the CCNB accumulation and the states of RSK. The CDK1 abundance was used as an internal control. As shown in Figure 1.4, Flag signals were detected from 6 h of culture and increased at 9 h in both Flag-*EMI1* mRNA-injected and Flag-*EMI2* mRNA-injected oocytes. At 24 h of culture, both Flag signal intensities were decreased and the signal of Flag-*EMI1* was hardly detected, while Flag-*EMI2* was still fairly detectable. CCNB1 had already accumulated at 6 h of culture in both Flag-*EMI* expressed oocytes and was increased at 9 h only in the Flag-*EMI1* mRNA-injected oocytes, whereas CCNB1 was first detected at 24 h in the no-injection oocytes. A band shift of RSK was detected at 9 h only in the Flag-*EMI1* expressed oocytes, whereas a clear upward shift was detected in all experimental groups at 24 h. CDK1 was almost unchanged throughout the culture periods. The CCNB1 accumulation and the upward shift of RSK bands all corresponded well with the observed GVBD rates.

The effect of EMI overexpression on GVBD was also assessed with oocytes

cultured with high cAMP concentration in order to see whether excess amounts of EMI could overcome cAMP-induced meiotic arrest (Fig.1.5). In the no-injection and the EGFP mRNA-injected oocytes, 5 mM 8-Br cAMP was able to stop GVBD for 48 h in most oocytes. The Flag-*EMI* mRNA-injected oocytes were able to override this condition and underwent GVBD. About 14.3% of the Flag-*EMI1*-expressing oocytes reached MII, whereas almost all the Flag-*EMI2*-expressing oocytes were arrested at MI.

(4) Effects of up- or downregulation of EMI after GVBD and MII arrest of porcine oocytes

The effect of EMI regulation after GVBD and MII arrest was investigated first with EMI overexpression. In the 48 h-cultured oocytes, the injection of either Flag-*EMI* mRNA inhibited oocyte maturation to different degrees; the Flag-*EMI1* mRNA injection resulted in 52.5% MI and 45.8% MII, whereas most of the Flag-*EMI2* mRNA-injected oocytes (97.9%) were arrested at MI (Fig.1.6A).

The effect of EMI downregulation on the oocyte meiotic progression after GVBD was also assessed by examining the nuclear states at 24 h and 48 h of culture was examined (Fig. 1.6B, C). At 24 h of culture, the majority of the *EMI2* asRNA-injected oocytes were at MI as EGFP mRNA-injected oocytes (67.0% and 85.9%, respectively). However, most of the *EMI1* asRNA-injected oocytes were at PMI and the MI rate (24.0%) was significantly lower than those of other experimental groups, confirming the delay of meiotic resumption and subsequent progression from PMI to MI in the *EMI1* downregulated oocytes. Corresponding with this, although 98.6% of EGFP mRNA-injected oocytes completed maturation, only 32.4% of *EMI1* downregulated oocytes reached MII and 36.5% remained at MI at 48 h of culture. Importantly, most of the *EMI2* asRNA-injected oocytes formed PN (94.9%) and none were at MII. In contrast, no *EMI1*

asRNA-injected oocytes had formed PN at 48 h of culture as well as EGFP mRNA-injected oocytes (Fig. 1.6C). A representative image of a PN in *EMI2* asRNA-injected oocyte is shown in Figure 1.6D.

The delayed GVBD and meiotic progression by the *EMI1* downregulation together with the PN formation by the *EMI2* downregulation were confirmed by Western blotting analysis shown in Figure 1.7. In the no-injection and *EMI2* asRNA-injected oocytes, CCNB1 had accumulated at 24 h and a similar degree of accumulation was detected at 48 h. For the *EMI1* asRNA-injected oocytes, although the CCNB1 accumulation at 48 h was comparable with that of the no-injection oocytes, the amount at 24 h was much lower than those of the no-injection and *EMI2* asRNA-injected oocytes. The upward shift of RSK was observed from 24 h of culture in all experimental groups, and it remained shifted upward until 48 h in the no-injection and *EMI1* asRNA-injected oocytes but had shifted downward at 48 h in the *EMI2* asRNA-injected oocytes, indicative of the release from MII.

Since the involvement of EMI in MII arrest and its role as CSF have been emphasized in *Xenopus* and mouse oocytes, the effects of EMI on MII maintenance and PN formation at 24 h after the parthenogenetic activation of MII oocytes were evaluated. For this experiment, Flag-*EMI* mRNA was injected to MII oocytes because the most oocytes injected with Flag-*EMI* mRNA at GV stage were unable to reach MII at 48 h of culture. The experimental time courses are indicated in Figure 1.8A. As shown in Figure 1.8B, the majority of no-injection, EGFP mRNA-injected, and Flag-*EMI1* mRNA-injected oocytes formed a PN (87.8%, 89.7% and 79.2%, respectively), whereas significantly fewer Flag-*EMI2* mRNA-injected oocytes formed PN (12.8%). Next, I compared the accumulation of Flag-EMI protein and the states of CCNB1, RSK, and CDK1 in the oocytes treated as follows: mRNA injected at the GV stage and cultured for 6 h (GV sample; Fig.

1.8Aa), injected at MII and cultured for 6 h (MII sample; Fig. 1.8Ab), and MII sample parthenogenetically activated and cultured for 24 h (activated sample; Fig. 1.8Ac). The no-injection oocytes were also collected at the same time points without mRNA injections and the results were shown in Figure 1.8C. The Flag-EMI1 expression was very low in the MII sample compared to the GV sample and was undetectable in the activated sample. In contrast, Flag-EMI2 expression was detectable in activated sample as well as in MII sample, although the level was lower than that of the GV sample. The CCNB1 accumulation was confirmed in the MII and activated samples of all experimental groups including the no-injection oocytes. The RSK bands were shifted upward in the MII samples in all experimental groups, and it remained shifted up in 72 h only in the Flag-*EMI2* mRNA-injected oocytes with the parthenogenetic activation stimulus. The bands had shifted downward in the activated sample in the Flag-*EMI1* mRNA-injected and no-injection oocytes. The CDK1 signals were unaffected in all the samples. The intensity of CCNB1 in the MII samples of the Flag-*EMI* mRNA-injected oocytes was quantified relative to each no-injection oocyte (Fig. 1.8D). The Flag-*EMI2* mRNA-injected oocytes displayed relatively high CCNB1 intensity levels compared to the Flag-*EMI1* mRNA-injected oocytes.

Discussion

In this chapter, I investigated the functions and roles of porcine EMI during oocyte maturation focusing especially on GVBD and MII arrest. First, the effects on GVBD was investigated. When EMI1 or EMI2 was overexpressed, both resulted in an early accumulation of CCNB and caused precocious GVBD. The function of EMI in the inhibition of CCNB degradation by blocking APC/C activity has been reported in *Xenopus* and mouse oocytes (Ohsumi et al., 2004; Madgwick et al., 2006; Marangos et al., 2006; Ohe et al., 2007), and current findings suggest that this is also the case in porcine oocytes. The results in porcine oocytes are consistent with those described for mouse oocytes, in which the overexpression of GFP-hEMI1 accelerated the GVBD (Marangos et al., 2006).

The precocious GVBD caused by EMI overexpression was observed even when the oocytes were cultured in the presence of cAMP-supplemented culture medium, which maintains oocytes at the GV stage by maintaining a high cAMP level and mimicking the follicular environment. The results obtained in this chapter agree with those in mouse oocytes, which indicated that EMI could accumulate CCNB in a high-cAMP environment created with a cAMP phosphodiesterase inhibitor, IBMX (Marangos et al., 2006). These results further indicate the constant synthesis of a small amount of CCNB in GV oocytes within ovarian follicles and they highlight the importance of CCNB degradation via APC/C in these follicular oocytes for the maintenance of GV arrest.

Furthermore, in this chapter, it revealed several differences between the functions of EMI1 and EMI2. Although an excess amount of either EMI initiated early GVBD, the exact culture period until GVBD slightly differed between the two; 9 h for EMI1-overexpressed oocytes and 12 h for EMI2-overexpressed oocytes. This implies that the APC/C inhibitory effect of EMI1 is more effective than that of EMI2 at this culture period. APC/C is known to require an activation factor, either Cdh1 or Cdc20, for its

activation. Various studies noted that EMI1 has the ability to interact with APC/C activated by both Cdh1 and Cdc20 whereas EMI2 interact mainly with APC/C activated by Cdc20 (Miller et al., 2006; Tang et al., 2010). It was reported that in mouse and porcine oocytes, only Cdh1 worked for APC/C activation during the GV stage and that the transition from Cdh1 to Cdc20 occurred around GVBD (Reis et al., 2006; Yamamuro et al., 2008). It can therefore be speculated that the difference in the abilities of EMI1 and EMI2 to promote GVBD is attributed to the difference in their interacting APC/C activators.

The effect of EMI downregulation on GVBD was analyzed by injecting *EMI* asRNA. As both porcine EMIs stimulated CCNB accumulation and accelerated GVBD, I expected that the downregulation of both EMI would slow down the CCNB accumulation and delay GVBD. However, the results clearly indicated that only the EMI1 downregulation had delayed the GVBD. In contrast to EMI1, EMI2 downregulation did not affect GVBD initiation or progression to MI, implying that EMI2 does not have a significant role during the GVBD to MI period. These results are compatible with the possible absence of EMI2 during these periods.

After GVBD, half of the EMI1 overexpressing oocytes reached MII whereas all of the EMI2 overexpression oocytes went into arrest at MI. This might be due to the stability differences between exogenous EMI1 and EMI2. Numerous studies of *Xenopus* and mouse oocytes have shown the instability of endogenous and exogenous EMI1 and its susceptibility to rapid degradation after GVBD (Ohsumi et al., 2004; Marangos et al., 2006). In contrast, EMI2 expression from early meiosis resulted in MI arrest in *Xenopus* oocytes (Ohe et al., 2007), and the present results showed that this is applicable to porcine oocytes as well. Consistent with this, the Western blotting analysis showed that at 24 h of culture, when most oocytes underwent GVBD, the exogenous EMI1 expression ceased whereas EMI2 was present. Although it was unable to detect endogenous EMI

and could not determine the actual expression levels of EMI within the oocytes, the results indicated the possible absence of EMI2 before MI in porcine oocytes. As for EMI1, it might also be required for the meiotic progression from PMI to MI in porcine oocytes, since many *EMI1* asRNA-injected oocytes remained at PMI whereas most of the no-injection and EGFP mRNA-injected oocytes reached MI. Similar PMI arrest was reported in mouse in which EMI1 was downregulated by morpholino-oligonucleotide (Marangos et al., 2006). That report indicated that the PMI arrest could possibly be triggered by the failure in metaphase spindle assembly and cannot be explained only by the accumulation of CCNB. Thus, further analyses are needed to clarify the causes of the PMI arrest in porcine EMI1 downregulated oocytes.

When EMI2, but not EMI1, was downregulated, it induced oocyte activation and PN formation. This coincides with the commonly noted characteristics and expression pattern of EMI2, which are noted in *Xenopus* and mouse; EMI2 started to be expressed after MI and worked as CSF in the initiation and maintenance of MII arrest (Liu and Maller, 2005; Schmidt et al., 2004; Tung et al., 2004; Nishiyama et al., 2007). The PN formation in the porcine EMI2 downregulated oocytes clearly showed the requirement of EMI2 in MII arrest in porcine oocytes, indicating that EMI2 function as CSF in porcine oocytes. The inhibition of parthenogenetic activation in the Flag-*EMI2* mRNA-injected MII oocytes further supports our assumption of porcine EMI2 being CSF. In contrast, Flag-*EMI1* mRNA injection to MII oocytes could not keep the oocytes at MII after the parthenogenetic activation, and this indicates that porcine EMI1 does not have a CSF function. The immunoblotting analysis revealed the immediate degradation of exogenous EMI1 compared with the 24-h persistency of exogenous EMI2 in the MII oocytes. In addition to this, the accumulated CCNB1 level was much higher in the *EMI2* mRNA-injected oocytes compared to the Flag-*EMI1* mRNA-injected oocytes. Thus, these results support

the speculation that EMI1 cannot either function or exist in MII oocytes.

In conclusion, from the finding in chapter 1, EMI1 and EMI2 was confirmed to exist in porcine oocytes and the porcine EMI seemed to share similar roles in GV oocytes to previously reported mouse EMI, which is able to accumulate CCNB and accelerate GVBD. In addition, porcine EMI2 functions as CSF in the MII oocytes as reported both in *Xenopus* and mouse oocytes. This is the first report showing EMI function in oocytes other than that of *Xenopus* and mouse.

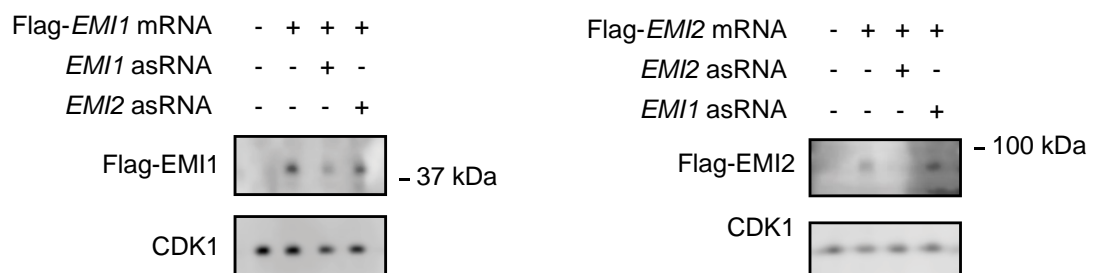


Fig.1.1 EMI overexpression and expression inhibition by Flag-*EMI* mRNA and *EMI* asRNA injection

Flag-EMI expression was detected by Western blotting 6 h after injection using an anti-Flag antibody. Effects of asRNA injection on EMI downregulation were examined by the injection of Flag-*EMI* mRNA with or without corresponding asRNA. Thirty oocytes were used for each lane.

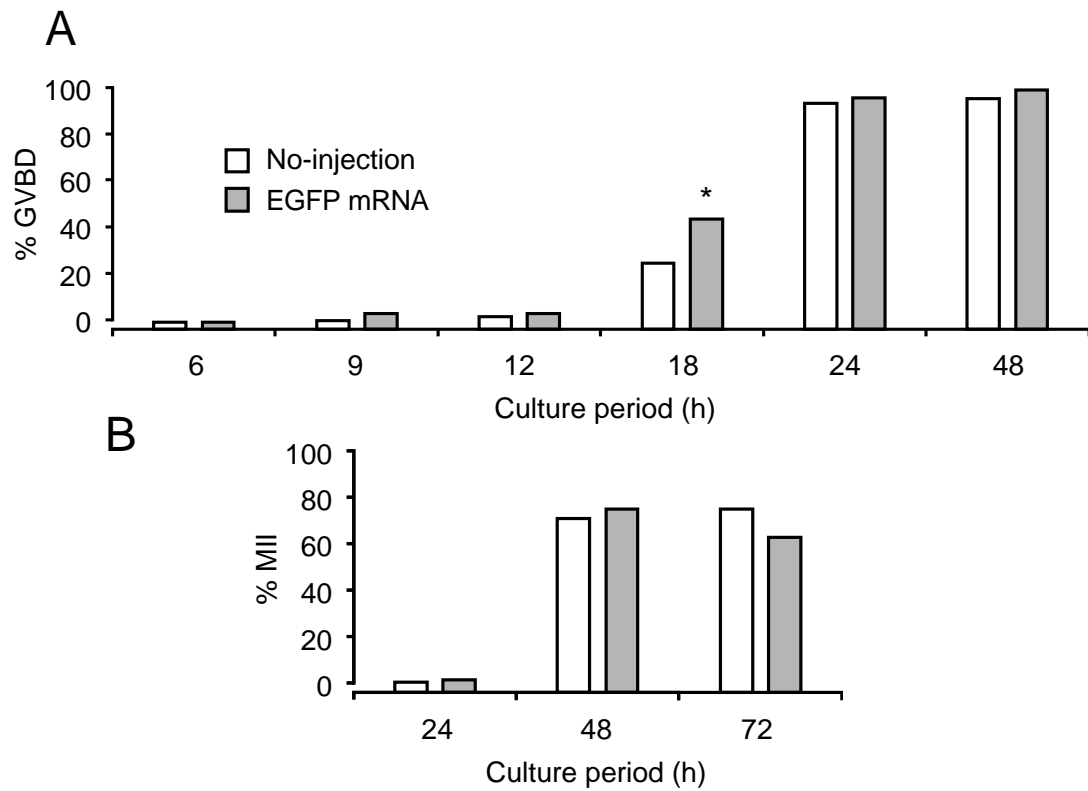


Fig.1.2 Influence of RNA injection on GVBD and MII rates in porcine oocyte
 GV oocytes injected with or without EGFP mRNA were cultured for the indicated periods, and GVBD rate (A) and MII rate (B) were calculated. At least two independent observations were performed and the total oocyte numbers of each bar were >30. * $p < 0.05$.

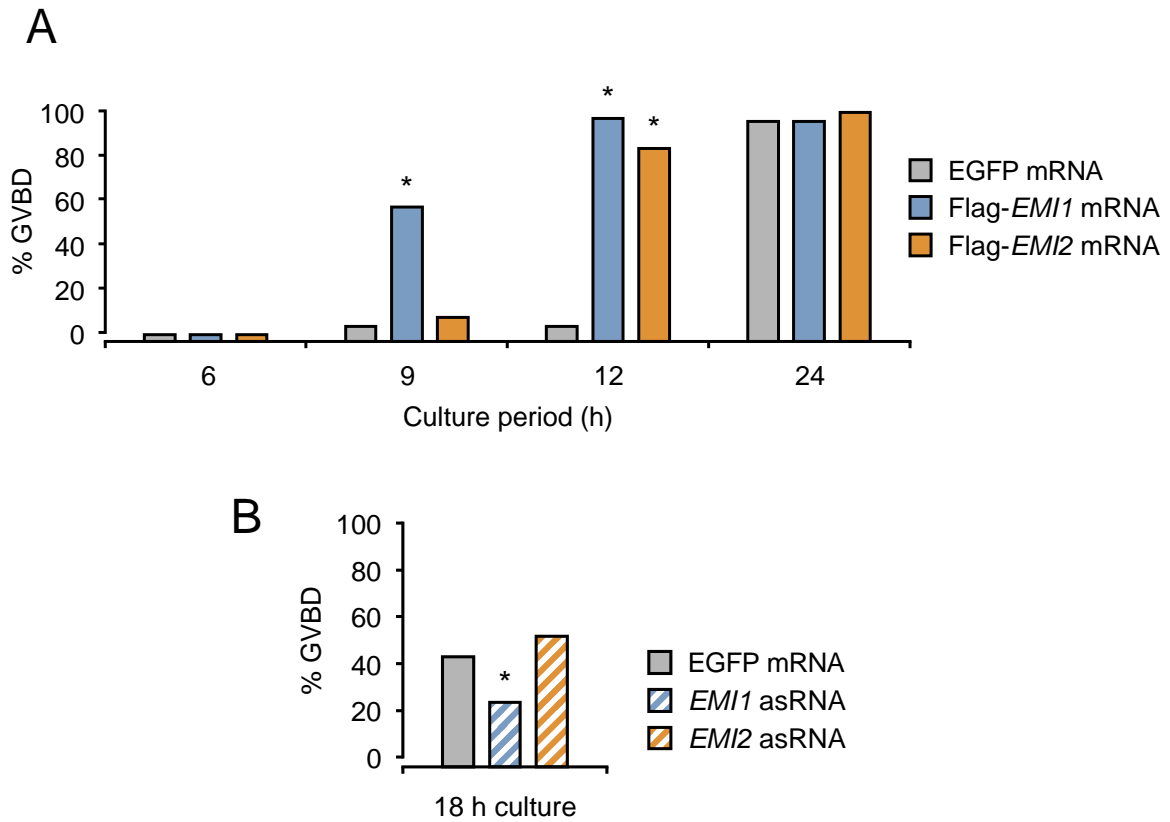


Fig.1.3 Effects of up- or downregulation of EMI on GVBD

GV oocytes injected with EGFP mRNA or Flag-*EMI* mRNA were cultured for the indicated periods and the oocyte's nuclear states were observed. (A) The GVBD rate was examined for Flag-*EMI* mRNA-injected oocytes at the indicated culture period. At least two independent experiments were performed and the total numbers of examined oocytes for each bar were >24 for 6 h and >55 for others. (B) The GVBD rates of EGFP mRNA and *EMI* asRNA-injected oocytes were examined at 18 h of culture. The experiments were repeated three times and more than 110 oocytes were examined for each bar.

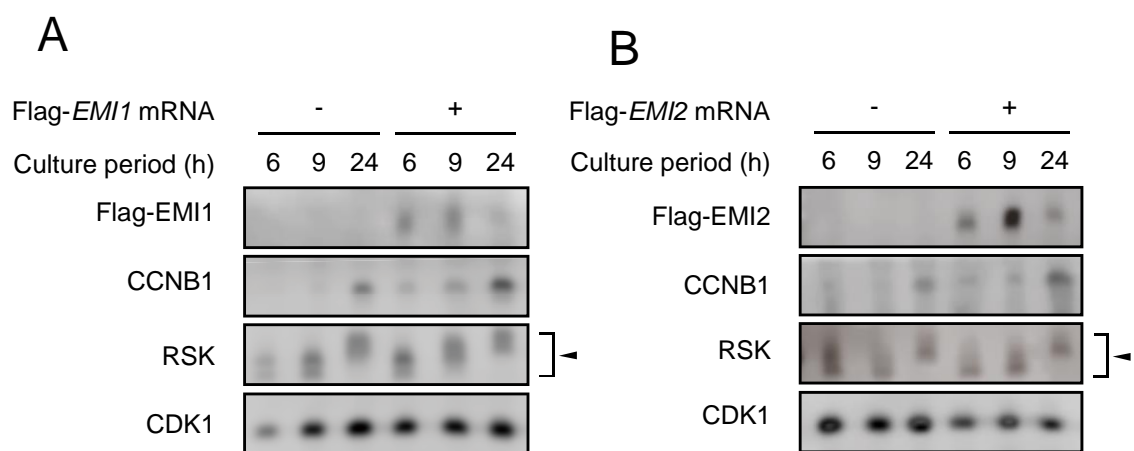


Fig.1.4 Western blotting analysis of Flag-EMI mRNA-injected oocytes

The states of CCNB1, RSK, and CKD1 were examined by Western blotting in (A) Flag-EMI1 mRNA- or (B) Flag-EMI2 mRNA-injected oocytes with no-injection oocytes. RNA injected or no-injection oocytes were cultured for indicated periods and subjected for Western blotting analyses using indicated antibodies. Arrowhead indicates mobility shifts of RSK. The experiments were repeated twice and representative results are shown. Twenty-five oocytes were used for each lane.

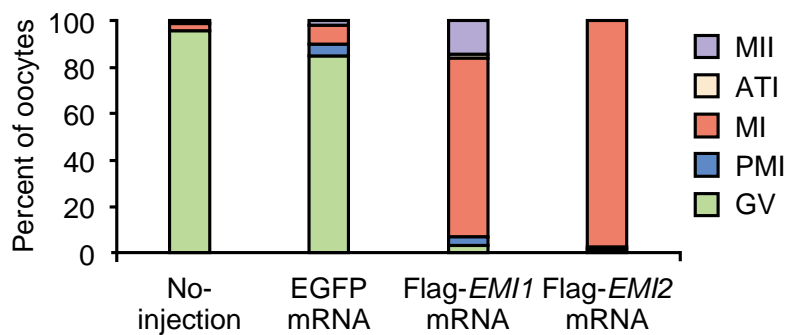


Fig.1.5 Effect of EMI overexpression on oocytes cultured in high cAMP concentration medium

Flag-*EMI* mRNA-, EGFP mRNA-injected and no-injected GV oocytes were cultured with 5 mM 8-Br cAMP for 48 h and the nuclear states were examined. Observed oocytes were categorized into the following: GV, germinal vesicle; GVBD, germinal vesicle breakdown; PMI, first meiotic prometaphase; MI, first meiotic metaphase; A-TI, first meiotic anaphase-telophase; MII, second meiotic metaphase. At least two independent experiments were performed and more than 60 oocytes were examined for each column.

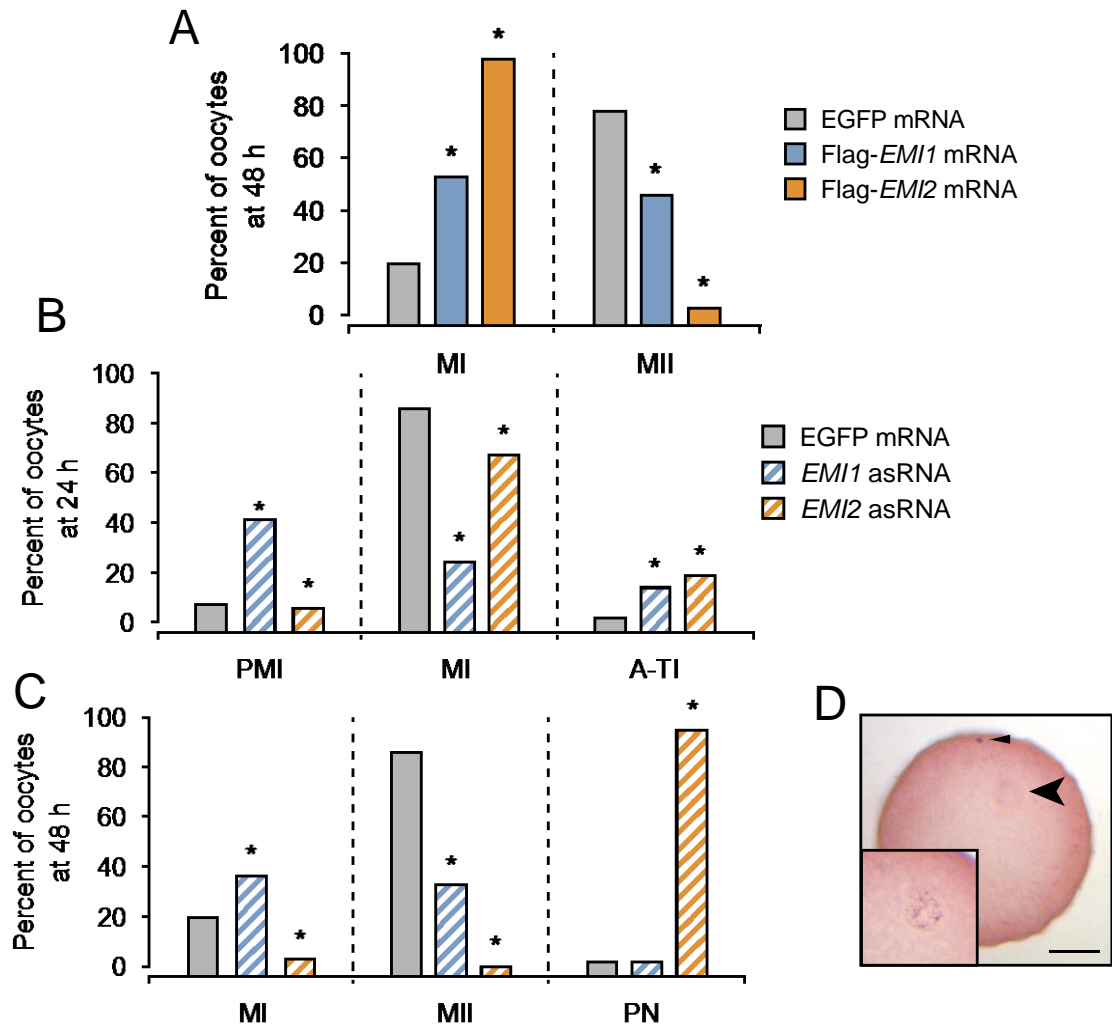


Fig.1.6 Effects of up- or downregulation of EMI after GVBD and MII arrest

GV oocytes injected with EGFP mRNA, Flag-*EMI* mRNA or *EMI* asRNA were cultured for 24 h or 48 h and the oocyte's nuclear states were observed. Oocytes from the following category was calculated: PMI, I, first meiotic prometaphase; MI, first meiotic metaphase; A-TI, first meiotic anaphase-telophase; MII, second meiotic metaphase; PN, pronucleus. (A) The oocytes were injected with Flag-*EMI* mRNA and percentage of MI and MII oocytes were examined at 48 h of culture. At least two independent experiments were performed and the total number of oocytes examined for each column was more than 60. (B, C) *EMI* asRNA-injected oocytes were cultured for 24 h (B) and 48 h (C), and the percentages of oocytes at indicated phases were examined. The experiments were repeated at least twice and more than 70 oocytes were used for each bar. * $p < 0.05$ compared to the EGFP mRNA-injected oocytes. (D) Representative image of PN observed in *EMI2* asRNA-injected oocytes cultured for 48 h. Inset: High-magnification image of PN. Arrow: PN. Arrowhead: polar body (PB) Scale bar, 50 μm .

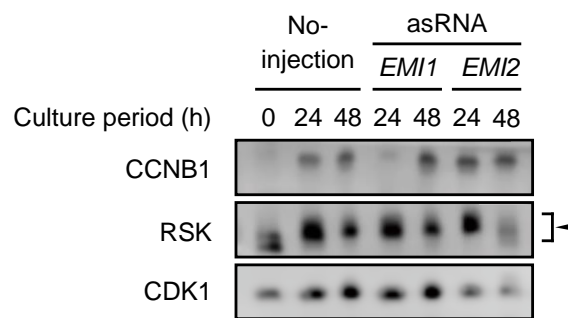


Fig.1.7 Western blotting analysis of EMI downregulated oocytes

The states of CCNB1, RSK, and CDK1 were examined by Western blotting analysis in *EMI1* asRNA- or *EMI2* asRNA-injected oocytes with no-injection oocytes. Antisense RNA injected or no-injection oocytes were cultured for indicated periods and subjected for Western blotting analyses using indicated antibodies. Arrowhead indicates mobility shift of RSK. Twenty-five oocytes were used for each lane.

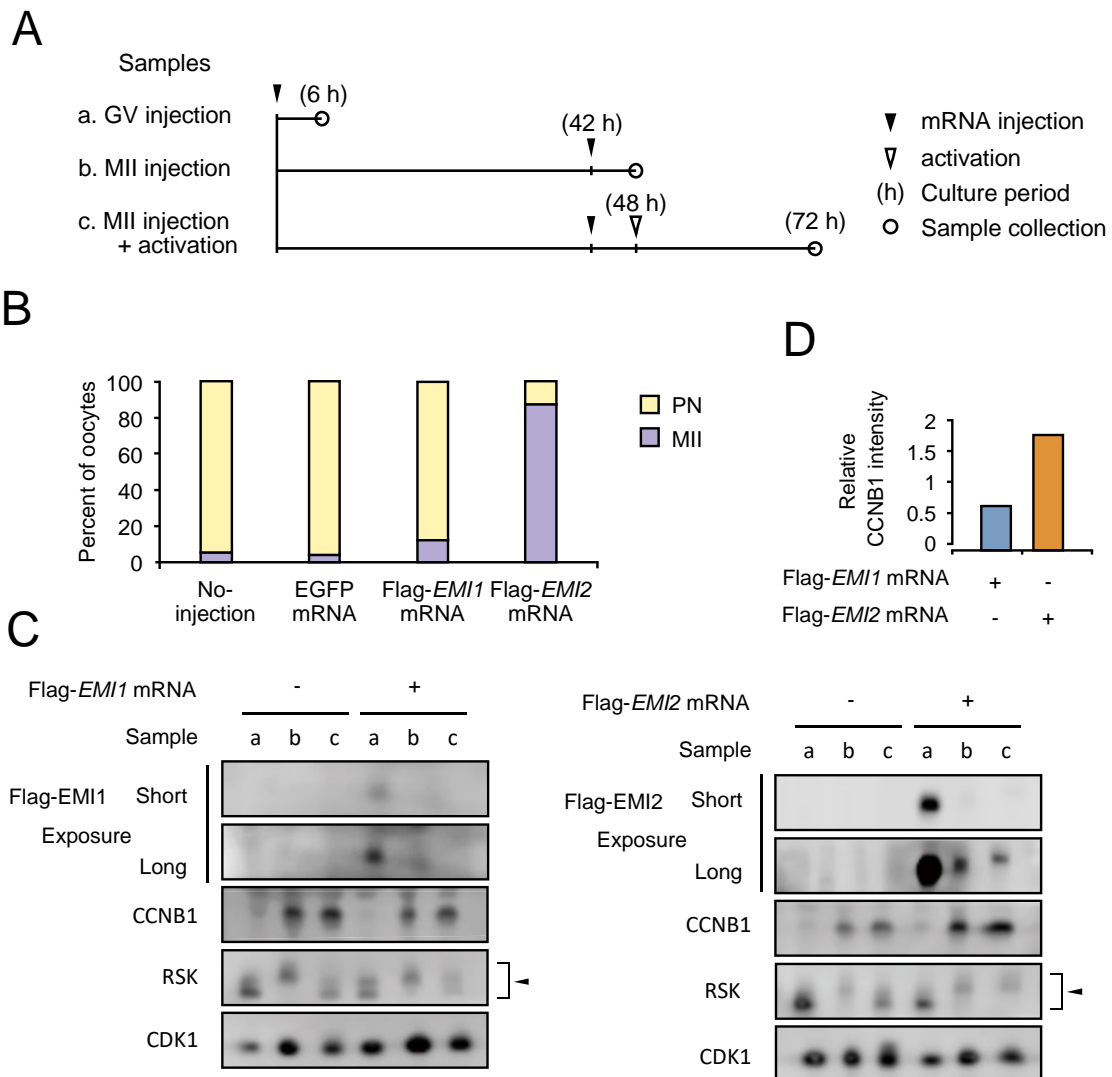


Fig.1.8 Effects of Flag-*EMI* mRNA injection into MII oocytes on PN formation after parthenogenetic activation.

(A) The schematic drawing of experimental time courses. The time-points of mRNA injection, activation, and oocyte collection were indicated. (B) The nucleus states of the sample c were observed and categorized into the following: MII, second meiotic metaphase and PN, pronucleus. More than 30 oocytes were examined for each bar. (C) Expression of Flag-EMI and the states of CCNB1, RSK, and CDK1 were evaluated by Western blotting. Samples a, b, and c are indicated in Fig.1.8A. Arrowhead indicates the mobility shift of RSK. Twenty-five oocytes were used for each lane. (D) The intensity of CCNB1 in Flag-*EMI* mRNA-injected sample b was quantified relative to each no-injection sample b from two independent Western blotting analyses.

Chapter 2

本章の内容は学術雑誌論文として出版する計画があるため、公表できない。5年以内
内に出版予定。

Chapter 3

本章の内容は学術雑誌論文として出版する計画があるため、公表できない。5年以内に出版予定。

General Discussion

本章の内容は学術雑誌論文として出版する計画があるため、公表できない。5年以内に出版予定。

Appendix

本章の内容は学術雑誌論文として出版する計画があるため、公表できない。5年以内に出版予定。

References

Ben-Eliezer I, Pomerantz Y, Galiani D, Nevo N, Dekel N. 2015. Appropriate expression of Ube2C and Ube2S controls the progression of the first meiotic division. *FASEB J.* 29(11):4670-81.

Chang DC, Xu N, Luo KQ. 2003. Degradation of cyclin B is required for the onset of anaphase in Mammalian cells. *J Biol Chem.* 278(39):37865-73.

Ciechanover A, Elias S, Heller H, Hershko A. 1982. "Covalent affinity" purification of ubiquitin-activating enzyme. *J Biol Chem.* 257(5):2537-42.

Corbin JD, Soderling TR, Park CR. 1973. Regulation of adenosine 3',5'-monophosphate-dependent protein kinase. I. Preliminary characterization of the adipose tissue enzyme in crude extracts. *J Biol Chem.* 248(5):1813-21.

Deshaies RJ, Joazeiro CA. 2009. RING domain E3 ubiquitin ligases. *Annu Rev Biochem.* 78:399-434.

Dimova NV, Hathaway NA, Lee BH, Kirkpatrick DS, Berkowitz ML, Gygi SP, Finley D, King RW. 2012. APC/C-mediated multiple monoubiquitylation provides an alternative degradation signal for cyclin B1. *Nat Cell Biol.* 14(2):168-76.

Draetta G, Luca F, Westendorf J, Brizuela L, Ruderman J, Beach D. 1989. Cdc2 protein kinase is complexed with both cyclin A and B: evidence for proteolytic inactivation of MPF. *Cell.* 56(5):829-38.

Dupré A, Buffin E, Roustan C, Nairn AC, Jesus C, Haccard O. 2013. The phosphorylation of ARPP19 by Greatwall renders the auto-amplification of MPF independently of PKA in *Xenopus* oocytes. *J Cell Sci.* 1;126(Pt 17):3916-26.

Eytan E, Ganoth D, Armon T, Hershko A. 1989. ATP-dependent incorporation of 20S protease into the 26S complex that degrades proteins conjugated to ubiquitin. *Proc Natl Acad Sci U S A.* 86(20):7751-5.

Fulka J Jr, Motlík J, Fulka J, Jílek F. 1986. Effect of cycloheximide on nuclear maturation of pig and mouse oocytes. *J Reprod Fertil.* 77(1):281-5.

Garnett MJ, Mansfeld J, Godwin C, Matsusaka T, Wu J, Russell P, Pines J, Venkitaraman AR. 2009. UBE2S elongates ubiquitin chains on APC/C substrates to promote mitotic exit. *Nat Cell Biol.* 11(11):1363-9.

Hampl A, Eppig JJ. 1995. Translational regulation of the gradual increase in histone H1 kinase activity in maturing mouse oocytes. *Mol Reprod Dev.* 40(1):9-15.

Han SJ, Chen R, Paronetto MP, Conti M. 2005. Wee1B is an oocyte-specific kinase involved in the control of meiotic arrest in the mouse. *Curr Biol.* 15(18):1670-6.

Han SJ, Conti M. 2006. New pathways from PKA to the Cdc2/cyclin B complex in oocytes: Wee1B as a potential PKA substrate. *Cell Cycle.* 5(3):227-31.

Hershko A, Heller H, Elias S, Ciechanover A. 1983. Components of ubiquitin-protein ligase

system. Resolution, affinity purification, and role in protein breakdown. *J Biol Chem.* 258(13):8206-14.

Hoffmann S, Tsurumi C, Kubiak JZ, Polanski Z. 2006. Germinal vesicle material drives meiotic cell cycle of mouse oocyte through the 3'UTR-dependent control of cyclin B1 synthesis. *Dev Biol.* 292(1):46-54.

Jin L, Williamson A, Banerjee S, Philipp I, Rape M. 2008. Mechanism of ubiquitin-chain formation by the human anaphase-promoting complex. *Cell.* 133(4):653-65.

Kirkpatrick DS, Hathaway NA, Hanna J, Elsasser S, Rush J, Finley D, King RW, Gygi SP. 2006. Quantitative analysis of in vitro ubiquitinated cyclin B1 reveals complex chain topology. *Nat Cell Biol.* 8(7):700-10.

Kim C, Xuong NH, Taylor SS. 2005. Crystal structure of a complex between the catalytic and regulatory (R1alpha) subunits of PKA. *Science.* 307(5710):690-6.

Kleiger G, Mayor T. 2014. Perilous journey: a tour of the ubiquitin-proteasome system. *Trends Cell Biol.* 24(6):352-9.

Kumagai A. and Dunphy WG. 1995. Control of the Cdc2/cyclin B complex in *Xenopus* egg extracts arrested at a G2/M checkpoint with DNA synthesis inhibitors. *Mol Biol Cell.* 6(2):199-213.

Kuroda T, Naito K, Sugiura K, Yamashita M, Takakura I, Tojo H. 2004. Analysis of the roles

of cyclin B1 and cyclin B2 in porcine oocyte maturation by inhibiting synthesis with antisense RNA injection. *Biol Reprod.* 70(1):154-9.

Liu J, Maller JL. 2005. Calcium elevation at fertilization coordinates phosphorylation of XErp1/Emi2 by Plx1 and CaMK II to release metaphase arrest by cytostatic factor. *Curr Biol* 15(16):1458-1468.

Madgwick S, Hansen DV, Levasseur M, Jackson PK, Jones KT. 2006. Mouse Emi2 is required to enter meiosis II by reestablishing cyclin B1 during interkinesis. *J Cell Biol* 11;174(6):791-801.

Marangos P, Verschuren EW, Chen R, Jackson PK, Carroll J. 2007. Prophase I arrest and progression to metaphase I in mouse oocytes are controlled by Emi1-dependent regulation of APC(Cdh1). *J Cell Biol* 176(1):65-75.

Masui Y, Markert CL. 1971. Cytoplasmic control of nuclear behavior during meiotic maturation of frog oocytes. *J Exp Zool.* 177(2):129-45.

Miller JJ, Summers MK, Hansen DV, Nachury MV, Lehman NL, Loktev A, Jackson PK. 2006. Emi1 stably binds and inhibits the anaphase-promoting complex/cyclosome as a pseudosubstrate inhibitor. *Genes Dev* 20(17):2410-2420.

Mochida S, Maslen SL, Skehel M, Hunt T. 2010. Greatwall phosphorylates an inhibitor of protein phosphatase 2A that is essential for mitosis. *Science* 330(6011):1670-3.

Naito K, Fukuda Y, Toyoda Y. 1988. Effects of porcine follicular fluid on pronucleus formation in porcine oocytes matured in vitro. *Gamete Res.* 21:289-295.

Naito K, Kagii H, Iwamori N, Sugiura K, Yamanouchi K, Tojo H. 1999. Establishment of a small-scale Western blotting system named as "micro-Western blotting" for mammalian ova analysis. *J Mamm Ova Res.* 16:154-157.

Nishimura T, Fujii W, Kano K, Sugiura K, Naito K. 2012. Analyses of the involvement of PKA regulation mechanism in meiotic incompetence of porcine growing oocytes. *Biol Reprod.* 87(3):53.

Nishimura T, Fujii W, Sugiura K, Naito K. 2014. Cytoplasmic anchoring of cAMP-dependent protein kinase (PKA) by A-kinase anchor proteins (AKAPs) is required for meiotic arrest of porcine full-grown and growing oocytes. *Biol Reprod.* 90(3):58.

Nishimura Y, Kano K, Naito K. 2010. Porcine CPEB1 is involved in Cyclin B translation and meiotic resumption in porcine oocytes. *Anim Sci J.* 81(4):444-52.

Nishiyama T, Ohsumi K, Kishimoto T. 2007. Phosphorylation of Erp1 by p90rsk is required for cytosolic factor arrest in *Xenopus laevis* eggs. *Nature.* 446(7139):1096-9.

Ohashi S, Naito K, Kiu J, Sheng Y, Yamanouchi K, Tojo H. 2001. Expression of exogenous proteins in porcine maturing oocytes after mRNA injection: kinetic analysis and oocyte selection using EGFP mRNA. *J of Reprod and Dev.* 47(6): 351-357

Ohashi S, Naito K, Sugiura K, Iwamori N, Goto S, Naruoka H, Tojo H. 2003 Analyses of mitogen-activated protein kinase function in the maturation of porcine oocytes. *Biol. Reprod.* 68(2):604-609.

Ohe M, Inoue D, Kanemori Y, Sagata N. 2007. Erp1/Emi2 is essential for the meiosis I to meiosis II transition in *Xenopus* oocytes. *Dev Biol* 303(1):157-164.

Ohsumi K, Koyanagi A, Yamamoto TM, Gotoh T, Kishimoto T. 2004. Emi1-mediated M-phase arrest in *Xenopus* eggs is distinct from cytostatic factor arrest. *Proc Natl Acad Sci U S A* 101(34):12531-12536.

Peters JM. 2002. The anaphase-promoting complex: proteolysis in mitosis and beyond. *Mol Cell.* 9(5):931-43.

Reis A, Chang HY, Levasseur M, Jones KT. 2006. APC^{Cdh1} activity in mouse oocytes prevents entry into the first meiotic division. *Nat Cell Biol.* 8(5):539-40.

Sagata N. 1996. Meiotic metaphase arrest in animal oocytes: its mechanisms and biological significance. *Trends Cell Biol.* 6(1):22-8.

Sako K, Suzuki K, Isoda M, Yoshikai S, Senoo C, Nakajo N, Ohe M, Sagata N. 2014. Emi2 mediates meiotic MII arrest by competitively inhibiting the binding of Ube2S to the APC/C. *Nat Commun.*28;5:3667.

Schmidt A, Duncan PI, Rauh NR, Sauer G, Fry AM, Nigg EA, Mayer TU. 2005. *Xenopus*

polo-like kinase Plx1 regulates XErp1, a novel inhibitor of APC/C activity. *Genes Dev* 19(4):502-513.

Schultz RM, Wassarman PM. 1977. Biochemical studies of mammalian oogenesis: Protein synthesis during oocyte growth and meiotic maturation in the mouse. *J Cell Sci.* 24:167-94.

Shimaoka T. 2010. Ph.D dissertation: Analysis of the function of Wee1B on GV arrest. [in Japanese]. Graduate School of Agricultural and Life Sciences, The University of Tokyo.

Shoji S, Yoshida N, Amanai M, Ohgishi M, Fukui T, Fujimoto S, Nakano Y, Kajikawa E, Perry AC. 2006. Mammalian Emi2 mediates cytostatic arrest and transduces the signal for meiotic exit via Cdc20. *EMBO J* 25(4):834-845.

Tang W, Wu JQ, Chen C, Yang CS, Guo JY, Freel CD, Kornbluth S. 2010. Emi2-mediated inhibition of E2-substrate ubiquitin transfer by the anaphase-promoting complex/cyclosome through a D-box-independent mechanism. *Mol Biol Cell* 21(15):2589-2597.

Tung JJ, Hansen DV, Ban KH, Loktev AV, Summers MK, Adler JR 3rd, Jackson PK. 2005. A role for the anaphase-promoting complex inhibitor Emi2/XErp1, a homolog of early mitotic inhibitor 1, in cytostatic factor arrest of *Xenopus* eggs. *Proc Natl Acad Sci U S A* 102(12):4318-4323.

Voets E, Wolthuis RM. 2010. MASTL is the human orthologue of Greatwall kinase that

facilitates mitotic entry, anaphase and cytokinesis. *Cell Cycle*. 9(17):3591-601.

Wu T, Merbl Y, Huo Y, Gallop JL, Tzur A, Kirschner MW. 2010. UBE2S drives elongation of K11-linked ubiquitin chains by the anaphase-promoting complex. *Proc Natl Acad Sci U S A*. 107(4):1355-60.

Yamamuro T, Kano K, Naito K. 2008. Function of FZR1 and CDC20, activators of the anaphase-promoting complex, during meiotic maturation of swine oocytes. *Biol Reprod* 79(6):1202-9.

Ye Y, Rape M. 2009. Building ubiquitin chains: E2 enzymes at work. *Nat Rev Mol Cell Biol*. 10(11):755-64.

Acknowledgements

I would like to express my deepest appreciation to Dr. Kunihiko Naito for he has been supervising me for 2 years in my Master and 4 years in my Ph.D. He had provided me with many critical indications about my experimental results and showed me the direction which my study should be heading to. Addition to this, he had patiently and kindly watched me (probability with a lot of frustrations) perform experiments and stumble upon many difficulties. I would also like to express my appreciation to Dr. Koji Sugiura. Although he himself had his students to mentor, he had advised me of my doings and gave me many supports. I also would like to appreciate Dr. Wataru Fujii for advising me of my research, and I would like to thank Dr. Kazuhiro Chida, Dr. Yoshitsugu Matsumoto, and Dr. Satoshi Tanaka for reading and giving me advices about my dissertation.

I am also greatly thankful to the members of Lab of Applied Genetics. They had provided me with enjoyable time and had supported my life in laboratory. I also would like to thank the people at commercial slaughterhouse for making my visit to commercial slaughterhouse enjoyable. In addition, I want to thank Student Counseling Center and Psychiatric of Division for Health Service Promotion for supporting my laboratory life. I would not have been here if I hadn't had their support.

Last but not least, I would like to thank my family and my pet cockatiel for patiently watching me struggle my way through my research.